Electronic Supplementary Material (ESI) for Energy & Environmental Science.

Supporting Information

Structural Basis for Differing Electrocatalytic Water Oxidation by the Cubic, Layered and Spinel Forms of Lithium Cobalt Oxides

Graeme Gardner[a], Jafar Al-Sharab[b], Nemanja Danilovic[c], Yong Bok Go[a], Katherine Ayers[c], Martha Greenblatt[a] and G. Charles Dismukes[a,c]

[a] *Department of Chemistry and Chemical Biology, Rutgers, The State University of New Jersey, 610 Taylor Road, Piscataway, NJ 08854 USA E-mail: martha@chem.rutgers.edu; dismukes@rutger.edu*
[b] *Department of Engineering Technology, Northwestern State University, 205 Williamson Hall, Natchitoches, LA 71497 USA .*
[c] *Proton OnSite, 10 Technology Drive, Wallingford, CT 06492, USA*
[d] *Waksman Institute of Microbiology, Rutgers, The State University of New Jersey, 190 Frelinghuysen Road, Piscataway, NJ 08854 USA*

Experimental Details:

Catalyst Synthesis: Lithium cobalt oxide was synthesized via a sol-gel procedure. Equimolar amounts of $LiNO_3$ and $Co(NO_3)_2$•$6H_2O$ were mixed in an aqueous solution (volume ~30 mL) containing urea and citric acid. The Co:Citric acid and Co:Urea molar ratio was 1:2 for both. The aqueous solution was stirred at 85 °C until the water evaporated and a smooth gel was formed. The gel was further dried overnight at 170 °C to form a xerogel product, which was crushed and calcined for 4 hours at 400 or 700 °C. Co_3O_4 was also synthesized as a control with the same method, but leaving out the $LiNO_3$. The PXRD of the sample is given in Figure S9. The resulting powders were washed (sonicated) with H_2O and EtOH to remove residual organics or any soluble salts, and the crystallinity was confirmed by powder X-ray diffraction. PXRD was performed with a Bruker D8 Advance diffractometer (Bragg-Brentano geometry, Cu Kα radiation). Scanning electron microscopy was performed with a Zeiss Sigma field emission SEM with Oxford EDSLEO. A cross-sectional view of the catalyst films was prepared by drop-casting the ink used to make working electrodes onto an ITO-coated glass slide. The slide was scored and snapped across the film to create a cross-sectional view.

Electrochemistry: Electrochemical experiments were performed on one of 3 potentiostats – a CH Instruments 700C Biopotentiostat, a Solartron 1287 (equipped with 1255B FRA) potentiostat/galvanostat, or a PAR 2263 potentiostat/galvanostat. Working electrodes were prepared by drop-casting 5 μL of a catalyst ink (metal oxide powder/acetylene black/Nafion®(117)) onto a homemade glassy carbon electrode (HTW SIGRADUR G glassy carbon disks fixed with epoxy into a G-10 Garolite rod). See **figure S1** for film morphology. The inks were ~12 mg/mL LT-$LiCoO_2$ or 42 mg/mL HT-$LiCoO_2$, 25% by mass conductive carbon (acetylene black, STREM Chemicals) and 0.67% by mass Nafion® in mixed water/ethanol solvent. Electrode pellets made of catalyst, carbon, and PVDF were constructed for use in long term experiments, as the Nafion-based film is unstable to bubble degradation over time (see **figure S7**). The pellet composition was 75% catalyst, 7.5% acetylene black, 7.5% graphite, and 10% polyvinylidene fluoride (PVDF) – average pellet weight was 6 mg. Pellets were pressed at 100,000 psi for 30 min and vacuum dried at 140 °C overnight. A back contact to a Ti foil was made with a small amount of silver paint, and the whole electrode was sealed with epoxy. Electrolytes were 1 M NaOH (NaOH poellets, Sigma-Aldrich, reagent grade, ≥98%) for alkaline conditions and 1 M buffer strength phosphate prepared from NaH_2PO_4 and K_2HPO_4 (Sigma-Aldrich, ACS reagent, ≥98%). We used a CHI Hg/HgO (1 M NaOH, 0.140 V vs. NHE) reference electrode for basic conditions and a homemade Ag/AgCl (sat'd KCl, between 0.200-0.235 V vs. NHE) reference for neutral conditions calibrated against the NHE. Cyclic Voltammetry was performed to generate CV's shown in **figures S2**, and polarization curves (**figure 3**, main text). Typically, the scan rate was either 5 or 10 mV/sec, except for double-layer capacitance determinations, in which the scan rate was varied between 10 mV/sec and 200 mV/sec over a small window where no Faradaic current was observed (usually 200 mV wide). The scan rate dependence of capacitive current is shown in **figure S3**. Chronopotentiometry was performed for all catalyst films at 1 and 10 mA/cm^2 in both pH regimes.

Faradaic Efficiency: Faradaic efficiency measurements were performed in custom made glass electrochemical cells with Ace glass fittings such that an airtight seal could be achieved with the electrodes in place. A working electrode with catalyst film and counter electrode (carbon or titanium wire) were sealed into the cell and a rubber septum was placed in one of the necks. The cells were purged with Ar gas for 30 minutes, and subsequently run at 10 mA/cm^2

(working electrode geometric area) for 2 hours in a two-electrode configuration in 1 M NaOH. A 200 µL sample of the headspace was injected into a GC (Perkin Elmer Clarus 680 GC with TCD detector (Ar carrier gas) operating at 40ºC). Experiments were performed at least 3 times and each individual test was sampled in triplicate.

HRTEM Analysis: HRTEM of catalyst samples was performed on a JEOL 2010F field emission TEM/STEM, acceleration voltage 20-200 kV with ZrO-W field emission source. The samples were prepared by dispersion nanoparticle suspensions onto lacey carbon grids. We analyzed pristine samples of low-temperature (400 °C) and high-temperature (700 °C) synthesized $LiCoO_2$ (sol-gel), and "post-catalysis" samples, which were prepared from powders of $LiCoO_2$ dispersed onto a 1 cm^2 titanium mesh which were run at 1 mA for 1 hour, followed by washing with water and sonicating in a small amount of EtOH to make a dispersion. Analysis of images was performed with Gatan Digital Micrograph, accompanied by the Difftools package.[1]

Corrosion Tests: Corrosion of Li and Co during electrocatalysis was analyzed by ICP-OES of the electrolyte solution. The normal working electrodes were made by drop-casting inks of the catalyst/carbon/Nafion mixture onto the standard glassy carbon electrodes (5 mm diameter). These were submerged in a small volume electrolyte (normally 8 mL). Chronopotentiometric experiments at 10 mA cm^{-2} were run for 2 hours. The electrolyte was pulled through syringe filters and acidified for analysis with nitric acid to make a ~5% HNO_3 solution. Standard series (250 ppb, 500 ppb… 5 ppm 10 ppm) were prepared from standards purchased from SPEX Certiprep for Mn, Co, Ni, and Li. We used a PerkinElmer Optima 7300 V for analysis.

$LiCoO_2$ performance as anode catalyst in MEA configuration in a non-proprietary 25cm^2, non-pressurized stack for short term testing and a proprietary 28cm^2 differential pressure capable cell stack (previously reported[2]) for long term unattended operation. The anode (IrO_x baseline or $LiCoO_2$) or cathode (Pt black) catalysts were airbrushed onto a stainless steel (anode) or carbon (cathode) Gas-Diffusion Layers (GDLs) at a loading of 2-3 mg/cm^2 in a polymeric ink vehicle. The operating conditions for the 25cm^2 tests were 50 °C, with 0 psi H_2 back pressure with DIW feed on the anode side (polarization curve, **figure 6A** of the main text). The operating conditions for the 28cm^2 tests were 35-50 °C, with 50 psi H_2 back pressure, the stack was fed deionized water with 1% $KHCO_3$ (long-term stability, **figure 6B** of the main text).

SI Figures:

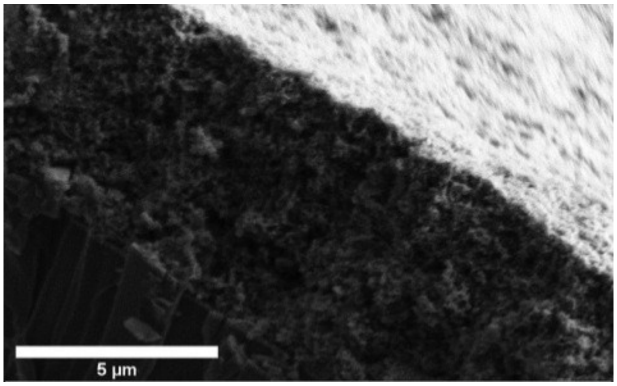

Figure S1. Cross-sectional SEM of catalyst composite films (on ITO glass) used to test electrochemical activity. The view is tilted slightly, with the bottom left-hand corner showing the underlying glass substrate, the dark rough portion illustrating the cross-section, and the lighter portion being the top of the film.

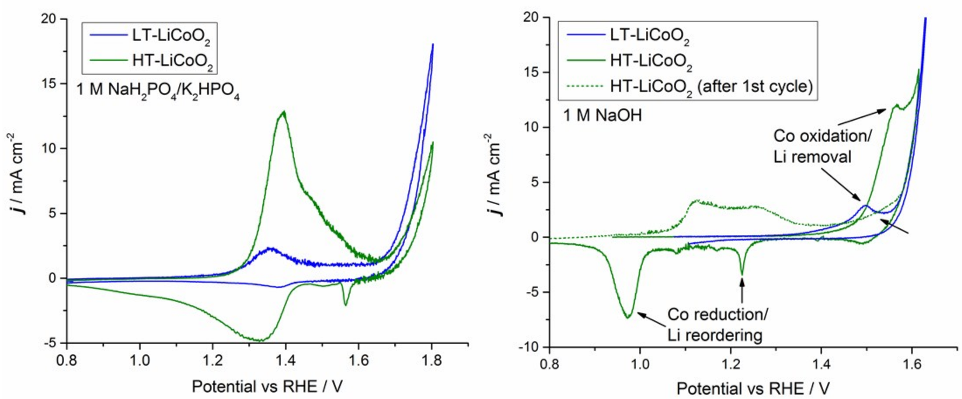

Figure S2. Cyclic voltammograms (10 mV sec^{-1}) of LT and HT-LiCoO$_2$ in both alkaline and neutral pH. Both illustrate distinct redox features before the onset of OER associated with Co oxidation and lithium removal/ordering, and in both cases the features diminish in yield on the cathodic sweep, suggesting irreversible chemical change.

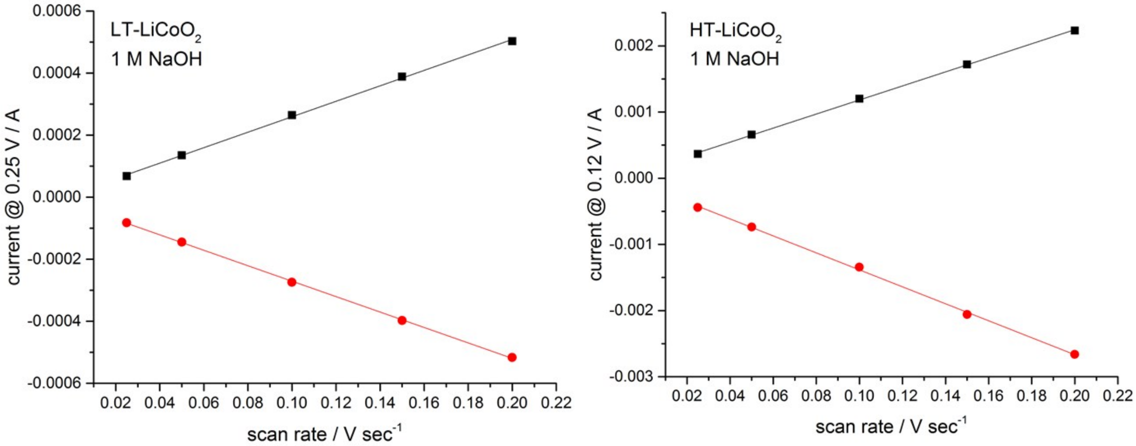

Figure S3. Scan rate dependence of capacitive current for LT and HT-LiCoO$_2$ in base. The C$_{dl}$ values are 2.5 and 11 mF for LT and HT, respectively.

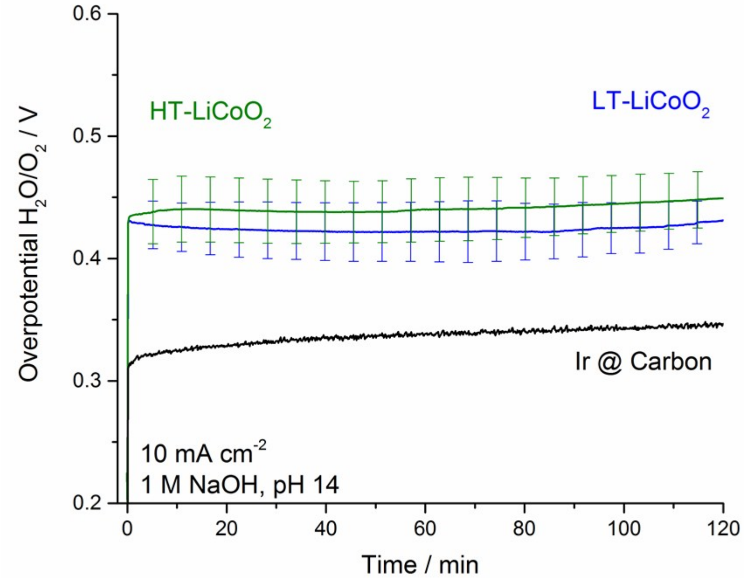

Figure S4. Chronopotentiometry of HT and LT-LiCoO$_2$ at 10 mA cm^{-2} in 1 M NaOH as compared to Ir nanoparticles.

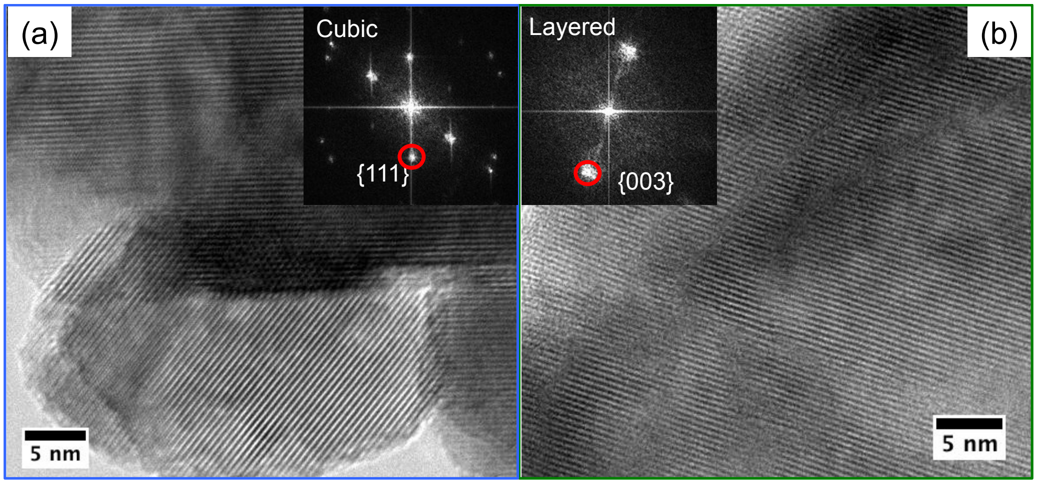

Figure S5. TEM images of the pristine (a) LT- and (b) HT- $LiCoO_2$ samples synthesized via sol gel method. The particles are well-faceted and lattice fringes are continuous from the interior to the surface of the sample. Insets show FFT patterns for whole image.

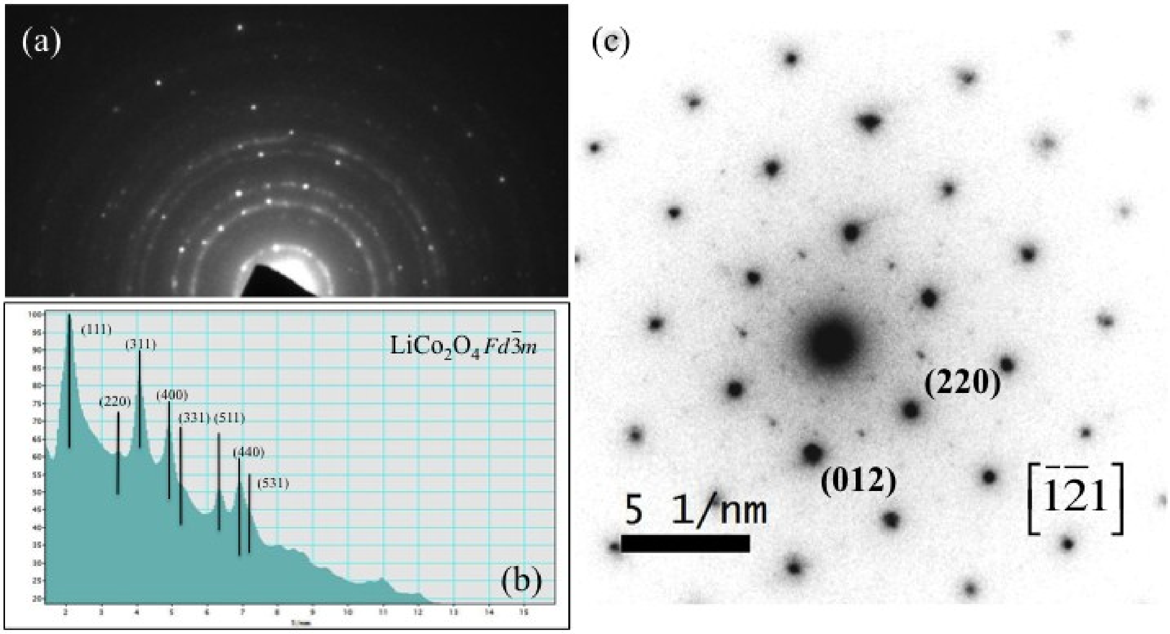

Figure S6. Selected area diffraction (SAD) analysis of (a) and (b) LT- and (c) HT-$LiCoO_2$ after electrolysis @ 10 mA cm^{-2} for 2 hours. The more nanoscrystalline LT-$LiCoO_2$ shows rings which can be rotationally averaged to yield the pattern in panel (b) that is indexed to spinel $LiCo_2O_4$ in cubic space group. In the case of HT-$LiCoO_2$, the main pattern is indexed to hexagonal $LiCoO_2$ ZA [-1-21], but faint reflections from the cubic spinel phase, including the 220 reflection are observed. (labels are on the lower right side of reflections).

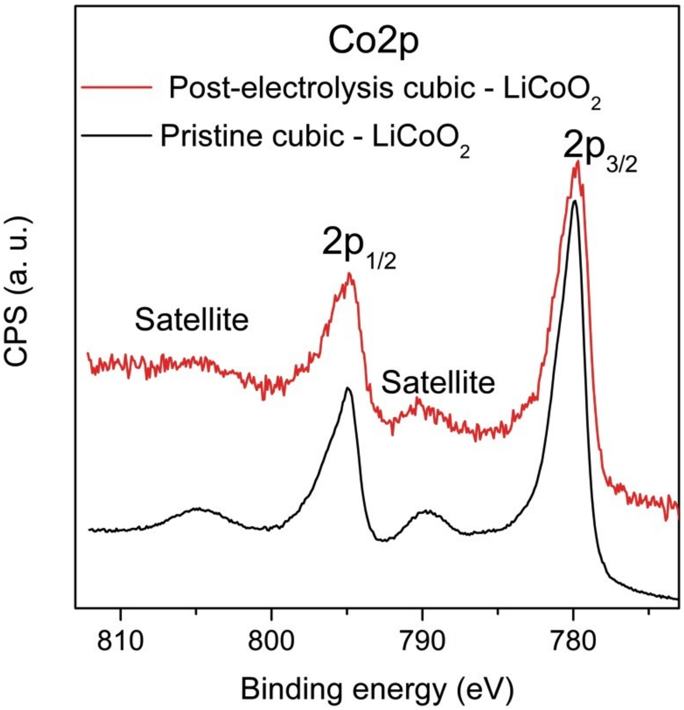

Figure S7. Co 2p XPS spectra of cubic LiCoO$_2$ before and after anodic electrolysis in the alkaline MEA electrolyzer that had been running for >1000 hours

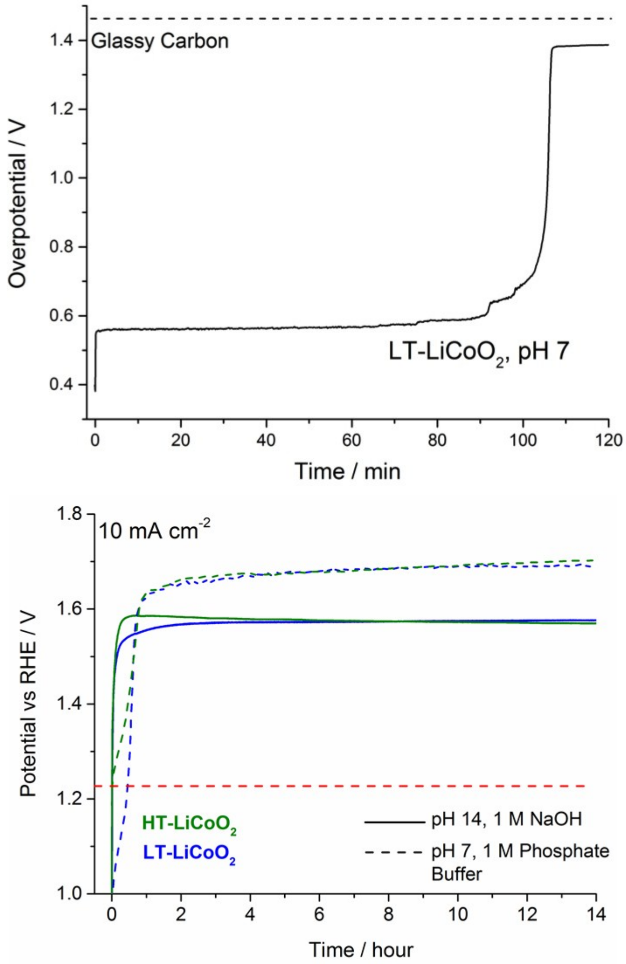

Figure S8. (a) Chronopotentiometry of LT-LiCoO$_2$ catalyst film containing Nafion® illustrating instability caused by film delamination over prolonged electrolysis. (b) Overnight stability @ 10 mA cm^{-2} on pellet electrodes

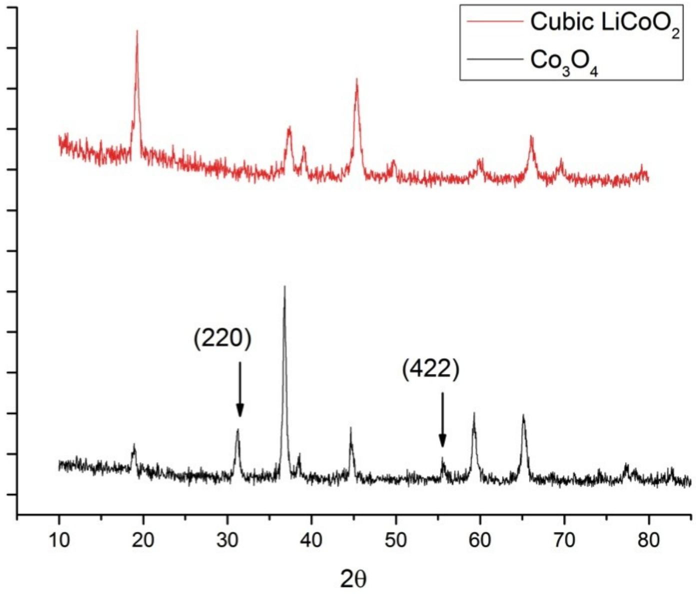

Figure S9. Powder X-ray diffraction pattern of Control Co_3O_4 catalyst. The space group (Fd-3m) is the same as that of cubic $LiCoO_2$ but the d-spacings and peak intensities change significantly – e.g. the absence of the 220 and 422 peaks present in the pristine $LiCoO_2$.

References:
1. D.R.G. Mitchell, *Microscopy Research and Technique*, 2008, **71**, 588-593
2. J. Parrondo, C.G. Arges, M. Niedzwiecki, E.B. Anderson, K.E. Ayers, V. Ramani, *RSC Advances*, 2014, **4**, 9875-9879